

A large, bold, black Roman numeral 'II' is centered within a white square, which is itself enclosed in a thick black border.

Publication II

V. Hynönen, T. Kurki-Suonio, W. Suttrop, R. Dux, K. Sugiyama, and the ASDEX Upgrade Team (2006). ASCOT simulations of fast particle effects on ASDEX Upgrade edge. In F. De Marco and G. Vlad (editors), *Proceedings of the 33rd European Physical Society Conference on Plasma Physics, Rome, Italy, June 19–23, 2006, Europhysics Conference Abstracts*, vol. 30I, P–2.151 (4 pp). European Physical Society.

© 2006 European Physical Society. By permission.

ASCOT simulations of fast particle effects on ASDEX Upgrade edge

V. Hynönen¹, T. Kurki-Suonio¹, W. Suttrop², R. Dux², K. Sugiyama³, and the ASDEX Upgrade Team²

¹ Association Euratom-Tekes, Helsinki University of Technology, Espoo, Finland

² Max-Planck-Institut für Plasmaphysik, EURATOM Association, Garching, Germany

³ Interdisciplinary Graduate School of Engineering Sciences, Kyushu Univ., Fukuoka, Japan

Introduction Fast ion behaviour in tokamak geometry deserves careful attention because 1) ions accelerated by external methods (RF, NBI) can cause significant damage on the material surfaces in today's machines, 2) in ITER, the fusion alphas have to be confined during slowing down, and 3) the edge fast ion population probably plays a significant role on the H-mode edge stability. Motivated by the ASDEX Upgrade quiescent H-mode (QH-mode) [1], originally discovered in DIII-D [2], we investigate the behaviour of neutral beam ions in the edge in the presence of collisions, magnetic ripple and radial electric field E_r . So far, the QH-mode has been obtained only with counter-injection of the neutral beams, and earlier ASCOT simulations have shown that with counter-injection, a significant fast ion population exists in the edge pedestal region [3]. In addition to beam ion behaviour also the flux of high-energy triton from beam-plasma D-D interactions onto the material surfaces is evaluated.

Wall and divertor load ASDEX Upgrade H-mode and QH-mode were compared by simulating 52 850 test particles corresponding to two counter-injected neutral beam lines with nominal injection energy $E = 60$ keV, particle fluence $\Gamma_{\text{NBI}} = 7.3 \times 10^{20} \text{ s}^{-1}$ and heating power 4.8 MW. The initial locations of the particles were calculated using the FAFNER code. The background data for the QH-mode simulations were extracted from the ASDEX Upgrade database for counter-injection discharge #17695 at $t = 5.6$ s. The corresponding virtual H-mode discharge was created by reversing the signs of the plasma current and toroidal magnetic field in the magnetic background data, and the sign of the pitch in the test particle data. All 8 combinations of co-/counter-injection, ripple/no ripple and E_r /no E_r were simulated.

Table 1 shows the breakdown of the particle fluence between the wall and the divertor. In the counter-injection simulations (QH-mode) the particles born on ill-confined orbits are lost promptly to the walls even without ripple, but in the co-injection simulations ripple is needed to create any notable wall load. Due to the prompt losses also the energy distributions of the wall losses are different: in counter-injection there are three peaks close full, half and one-third energy components of the nominal injection energy, whereas in co-injection the distribution is more continuous as are the divertor loads in all simulation.

Table 1: The breakdown of the particle fluence between the wall and the divertor. Percentages of the NBI source rate $\Gamma_{\text{NBI}} = 7.3 \times 10^{20} \text{ s}^{-1}$ are shown in parentheses.

Simulation	fluence/ 10^{19} s^{-1} (co-inj.)		fluence/ 10^{19} s^{-1} (counter-inj.)	
	wall	divertor	wall	divertor
No ripple, no E_r	0.03 (0.04%)	3.4 (4.6%)	6.9 (9.5%)	9.5 (13%)
Only E_r	0.1 (0.2%)	3.7 (5.1%)	8.7 (12%)	9.2 (13%)
Only ripple	2.8 (3.9%)	3.0 (4.0%)	12 (17%)	7.0 (9.6%)
Both ripple & E_r	1.8 (2.4%)	4.1 (5.6%)	11 (15%)	8.3 (11%)

Figure 1 shows the toroidal distribution of the wall load with ripple. Interestingly, in the co-injection case there is a clear peak halfway between the coils whereas in the counter-injection case the peak is only slightly left of each coil. The divertor load is uniform, and even the structure in the wall load disappears when $E_r \neq 0$.

Figures 3 and 4 show the particle flux onto the material surfaces for co- and counter-injection, respectively. The wall and divertor coordinates used in the figures are illustrated in figure 2. In the co-injection case both ripple and E_r have little effect on the divertor load, and the wall load is increased locally at $s_w \approx 0.3 \text{ m}$ when E_r is introduced. In the counter-injection case the ripple decreases the divertor load and increases the wall load. The wall particle fluxes are artificially low because of the axisymmetric 2D wall used in ASCOT. In reality the fast particles hit only the limiter surfaces and predominantly the part which is closest to the plasma.

Fast ion edge distribution From the same simulations as the wall and divertor loads we also get the fast ion edge distribution. Figure 5 shows the radial density of fast ions in all 8 simulations. In the counter-injection cases (QH-mode) the density of fast ions in the edge pedestal region ($\rho \approx 0.95$) is always higher than in the corresponding co-injection simulations (H-mode). For this reason also the edge density gradient is steeper in the counter-injection case. The ripple always reduces the density, but for co-injected particles the density does not decrease at the very edge of the plasma ($\rho > 0.95$) whereas in the counter-injection cases the density is decreased equally throughout the shown region. Therefore the ripple decreases the density gradient in co-injection, but in counter-injection the gradient stays the same. The radial electric field reduces the effect of ripple in both simulation cases.

Tritium surface distribution The long-term tritium retention will be a critical issue in future fusion reactors. In D–D discharge machines the tritium distribution on the plasma-facing components has been found to be similar to the distribution of high-energy triton implantation [4]. The incoming triton flux onto the material surfaces was simulated with and without ripple, and

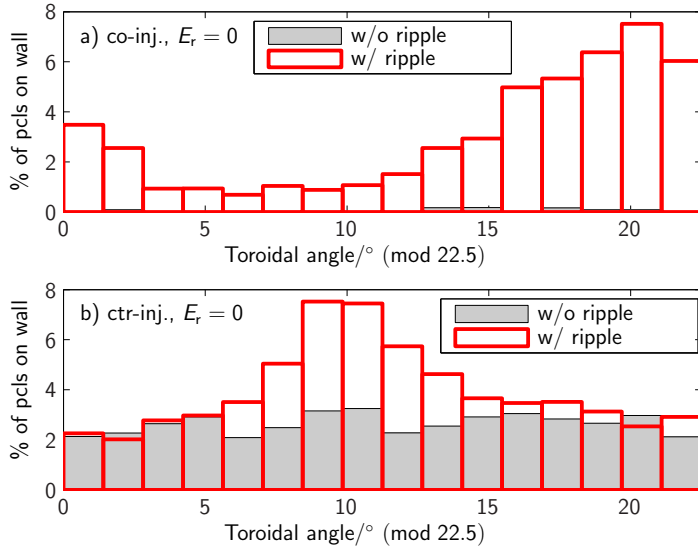


Figure 1: (Above) The toroidal distribution of the particle flux onto the wall as percentages of the total number of lost particles for a) co-injected neutral beams (H-mode) and b) counter-injected neutral beams (QH-mode) without E_r . Grey bars illustrate the results without ripple and red/grey thick-lined bars the results with ripple.

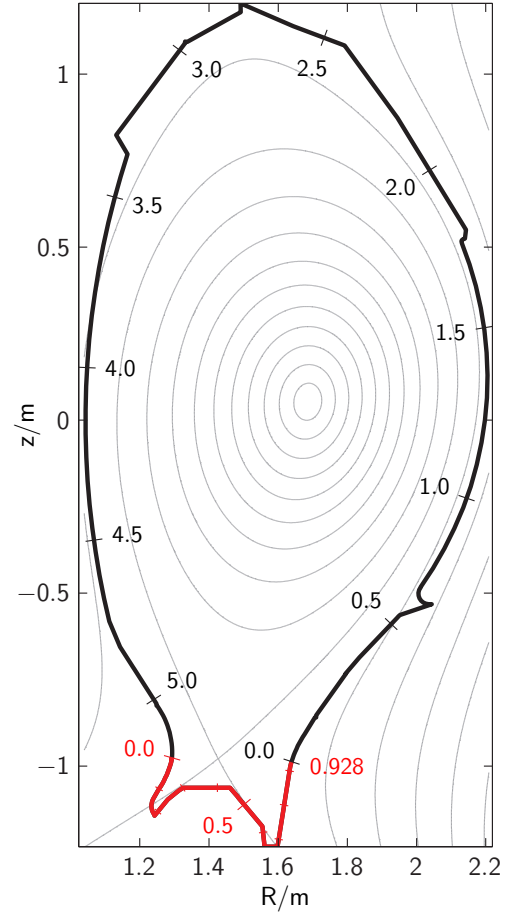


Figure 2: (Right) Illustration of the divertor and wall coordinates s_d (red/grey) and s_w (black), respectively.

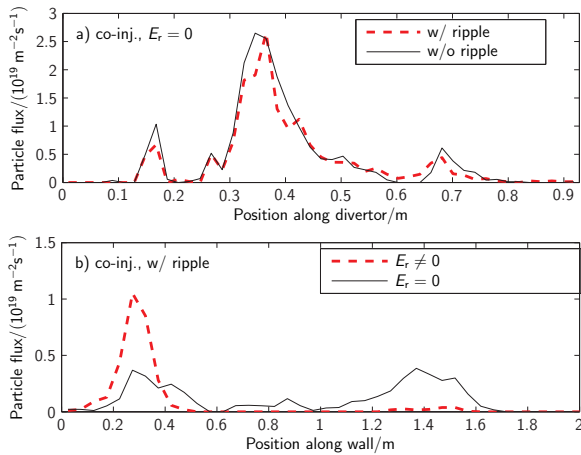


Figure 3: Co-NBI (H-mode): a) The particle flux onto the divertor with (red/grey thick ---) and without ripple (—) in the simulations without E_r . b) The particle flux onto the wall structures with (red/grey thick ---) and without E_r (—) in the simulations with finite toroidal ripple. Note that in b) only the range $s_w \leq 2.0$ is shown, because elsewhere the flux is zero.

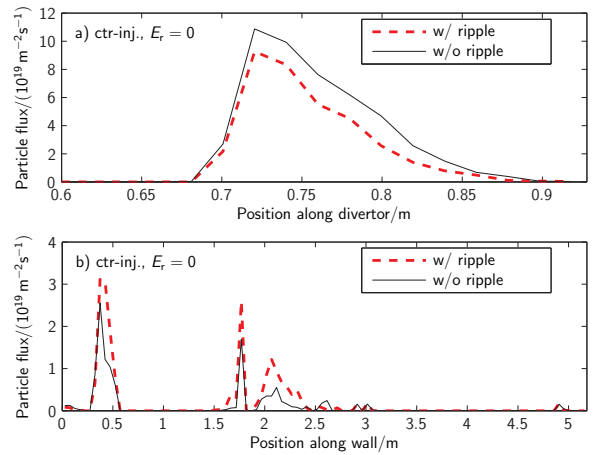


Figure 4: Counter-NBI (QH-mode): The particle flux a) onto the divertor and b) onto the wall with (red/grey thick ---) and without ripple (—) in the simulations without E_r . Note that in a) only the range $s_d \geq 0.6$ is shown, because elsewhere the flux is zero.

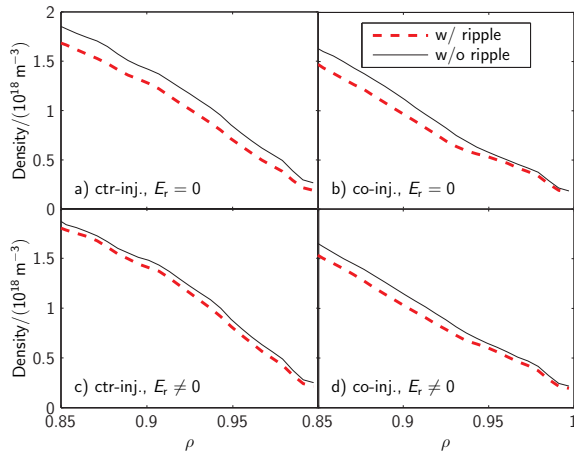


Figure 5: The radial density of fast ions with (---) and without ripple (—) in a) counter-injection, no E_r , b) co-injection, no E_r , c) counter-injection, $E_r \neq 0$, and d) co-injection, $E_r \neq 0$.

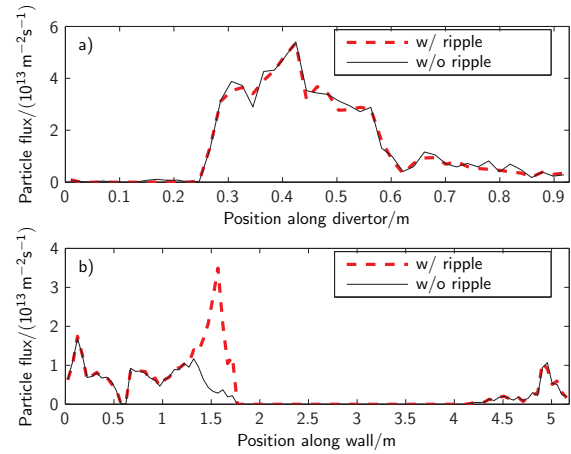


Figure 6: The triton flux a) onto the divertor and b) onto the wall structures in the axisymmetrical case (—) and in the case with finite toroidal ripple (red/grey thick ---).

in the axisymmetric case, 11% of all simulated tritons hit the divertor and 16% the wall. Introducing the ripple did not change the divertor load, but the wall load was increased up to 24% of the total number of particles. Figure 6 shows the triton flux onto the divertor and onto the wall. The divertor flux, indeed, is the same with and without ripple, but on the wall the flux onto the guard limiter ($s_w \approx 1.5$ m) is significantly higher with ripple. The simulation results are in qualitative agreement with preliminary measurements.

Conclusions In counter-injection the wall load is substantial even without toroidal ripple. The wall load is increased by the ripple, but the divertor load is either decreased (QH-mode) or is unchanged (H-mode). The effect of E_r alone is small, but together with ripple it decreases the effects of ripple. The fast ion density and the density gradient in the pedestal region are higher in counter-injection than in co-injection, and the ripple further reduces the gradient in co-injection.

Acknowledgements This work, supported by the European Communities, under the contract of Association between Association Euratom/Tekes, was carried out within the framework of the European Fusion Development Agreement. The views and opinions expressed herein do not necessarily reflect those of the European Commission. The computations presented in this document have been made with CSC's computing environment. CSC is the Finnish IT center for science and is owned by the Ministry of Education.

References

- [1] W. Suttrop et al. *Plasma Phys. Control. Fusion* **45** 1399–1416, 2003
- [2] K. H. Burrell et al. *Plasma Phys. Control. Fusion* **44** A253–A263, 2002
- [3] W. Suttrop et al. *Nucl. Fusion* **45** 721–730, 2005
- [4] K. Sugiyama et al. *J. Nucl. Mat.* **337–339** 634–638, 2005